

Photochemical CO₂ reduction using structurally controlled g-C₃N₄

James J. Walsh,^a Chaoran Jiang,^b Junwang Tang^{b*} and Alexander J. Cowan^{a*}

^{a.} Stephenson Institute for Renewable Energy, University of Liverpool, L69 7ZD, Liverpool, UK. Email: a.j.cowan@liv.ac.uk

^{b.} Department of Chemistry, University College London: junwang.tang@ucl.ac.uk

† Footnotes relating to the title and/or authors should appear here.

Electronic Supplementary Information (ESI) available: Full experimental procedures, supporting photocatalytic and emission studies. See DOI: 10.1039/x0xx00000x

Graphitic carbon nitride (g-C₃N₄) synthesised from a urea precursor is an excellent CO₂ reduction photocatalyst using [Co(bpy)_n]²⁺ as a co-catalyst. A five-fold increase in activity for the highly polymerised urea derived g-C₃N₄ is achieved compared to alternative precursors. Transient absorption, time-resolved and steady-state emission studies indicate that the enhanced activity is related to both an increased driving force for photoelectron transfer and a greater availability of photogenerated charges.

Increasing atmospheric CO₂ levels due to anthropogenic activity has brought carbon capture and carbon utilisation into the public consciousness and to the forefront of chemical research. The reduction of CO₂ to useful feedstocks or fuels such as CO, formic acid and methanol can be achieved through photochemical, electrochemical and thermal methods. The photochemical reduction of CO₂ is particularly attractive as when coupled to light driven water oxidation it offers a route to carbon based solar fuels. Whilst significant progress has been made in recent years towards the delivery of efficient semiconductor photocatalysts for water oxidation,¹ the development of a visible light active, scalable, stable, photocatalytic system for CO₂ reduction in the presence of water remains an un-realised goal.

g-C₃N₄ is an organic polymeric photocatalyst that has been intensely studied for photocatalytic hydrogen evolution^{2, 3, 4, 5, 6, 7, 8, 9} and to a lesser extent water oxidation,^{3, 10} since a landmark study in 2009.² The band gap of g-C₃N₄ (typically ca. 2.5 eV) enables visible light activity. In addition, g-C₃N₄ has been shown to be photochemically and mechanically stable and relatively facile to synthesise.^{11, 12} In addition a diverse range of approaches towards enhancing the visible light activity of g-C₃N₄ have been reported including g-C₃N₄/metal oxide heterojunctions,¹³ dye-sensitised g-C₃N₄¹⁴ and full photocatalytic water splitting z-schemes.¹⁵ Of particular significance to this study is that some of us have recently shown that platinumized g-C₃N₄ prepared from different precursors can have markedly different levels of photocatalytic activity, with a urea-derived material achieving an internal quantum efficiency (IQE) of 26.5 % for hydrogen production, greatly exceeding previously reported g-C₃N₄ photocatalysts.¹⁶ This very high level of photocatalytic activity, an order of magnitude greater than comparable materials prepared from different precursors, was found to correlate to an increased degree of polymerization and decreased proton concentration within the urea based g-C₃N₄.

In contrast to the substantial literature relating to hydrogen evolution there are a more limited number of studies examining the use of g-C₃N₄ for CO₂ reduction in the presence of water.^{17, 18, 19, 20, 21} One issue is that to overcome competitive proton reduction to H₂ in the presence of water a selective CO₂ reduction co-catalyst is required. Recently Maeda *et al.*, have developed a range of [Ru(bpy)(CO)₂Cl₂] derivatives (bpy = 2,2'-bipyridine) where modification of the 4,4' positions of bpy has enabled either direct or indirect binding to g-C₃N₄,²⁰

²¹ giving rise to a material that reduced CO₂ to formate with an apparent quantum yield (AQY) of 5.7% at 400 nm.²² Alternative approaches have explored the use of scalable co-catalysts on g-C₃N₄ including [Co(bpy)_n]²⁺.^{17, 18, 19} In these studies the co-catalyst, which is assembled *in-situ*, has been shown to be effective for CO production with an AQY of 0.25% at 420 nm and excellent selectivity.¹⁸ Whilst these reports clearly demonstrate the potential application of g-C₃N₄ for CO₂ reduction, to date there have been relatively few systematic studies on exploring the nature of the g-C₃N₄ used with each co-catalyst. Herein we examine a range of carbon nitrides, including the previously reported highly active urea derived g-C₃N₄,¹⁶ for CO₂ reduction. The simple *in-situ* prepared [Co(bpy)_n]²⁺ co-catalyst is chosen as it has been reported to be highly effective with a wide range of different light absorbers,¹⁹ making it an ideal test platform to explore the role of different g-C₃N₄ structures derived from a range of precursors. We report both an enhancement in the activity for a g-C₃N₄/[Co(bpy)_n]²⁺ mediated CO₂ reduction system and an improved overall understanding into the factors controlling the high levels of activity of urea derived g-C₃N₄ in reductive photochemistry.

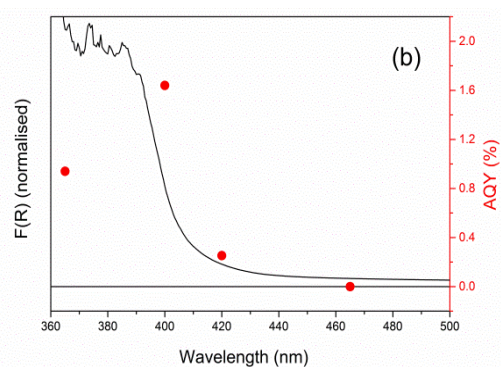
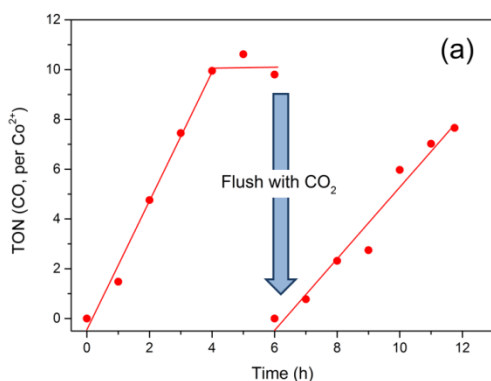
g-C₃N₄ was prepared from three different precursors (urea, thiourea and dicyandiamide (DCDA)) in the manner previously described, see ESI for full details.¹⁶ Previous reports on the g-C₃N₄/[Co(bpy)_n]²⁺ system have demonstrated successful CO₂ reduction in a solvent mixture of CH₃CN/H₂O with triethanolamine (TEOA) also being added as a sacrificial electron donor^{17, 18, 19} and the same solvent system is also employed here (CH₃CN:H₂O:TEOA, 3:1:1, 5 ml total). In the presence of urea derived g-C₃N₄ (2.5 mg), CoCl₂ (50 μmol dm⁻³), bpy (5 mmol dm⁻³) under an atmosphere of CO₂ we observe photocatalytic CO production with minimal H₂ evolution (CO:H₂, 3.3:1), see Table 1. In the absence of any one of these components CO₂ reduction does not occur (Table S1). A brief optimization of the concentrations of the catalyst components is presented in the ESI (Figs. S1, S2); however we highlight that the focus of this study is the optimization and mechanistic study of the g-C₃N₄ absorber. The lack of CO production in the absence of CO₂ is in-line with past isotope labelling studies which definitively confirmed CO₂ to be the carbon source for CO.¹⁸ The lack of CO₂ reduction in the absence of the bipyridine ligand is also in agreement with past electrochemical and photochemical studies of this co-catalyst, which has previously supported an assignment of the active catalyst precursor to a molecular species, proposed to be [Co(bpy)_n]²⁺.^{23, 24}

g-C ₃ N ₄ precursor	SSA (m ² .g ⁻¹) ^a	Band gap (eV)	CO rate μmol.g ⁻¹ .h ⁻¹ /TON ^b	H ₂ rate μmol.g ⁻¹ .h ⁻¹ /TON ^b	Selectivity (CO:H ₂)
Urea	43.8	2.9	460/9.2	138/2.8	3.3:1
Thiourea	18.5	2.5	22/0.4	86/1.7	0.25:1
DCDA	12.8	2.6	92/1.8	94/1.9	~ 1:1

Table 1: Photocatalytic activity for CO₂ reduction of the different g-C₃N₄ materials. Experiments carried out using 300 – 795 nm KG1 filter (Fig. S3), 40 mW.cm² illumination, 0.5 mg g-C₃N₄ per ml in CH₃CN/TEOA/H₂O (3:1:1), t = 2 h. ^a: Specific surface area, see reference 16; ^b: TON per Co²⁺ at t = 2 hours.

Under Xe lamp illumination (300 -795 nm) a turnover number (TON) per Co^{2+} of greater than 9 was achieved after 2 hours for CO production using urea derived g- C_3N_4 , Table 1. At prolonged periods it was found that the rate of CO_2 production began to decrease. To explore the factors limiting the TON experiments using a 400 nm LED were carried out, Fig. 1 (a). The use of a blue LED with a small spectral distribution allows for excitation of the g- C_3N_4 whilst avoiding the potential photochemical degradation of the reduced $[\text{Co}(\text{bpy})_n]^+$ ($\lambda_{\text{max}} \sim 600 \text{ nm}$).²⁴ After 6 hours of illumination at 400 nm the CO yield plateaued with a TON corresponding to ca. 10.6. Flushing the flask with fresh CO_2 leads to a recovery of activity and the system was able to achieve a TON > 18 before the experiment was terminated. This recovery in activity may indicate that a build-up of CO inhibits catalysis, either through CO interacting with the g- C_3N_4 , or more likely through inhibition of the co-catalyst. It is noted that CO inhibition has been previously reported during CO_2 photoreduction with other Co^{2+} catalysts.²⁵

Fig. 1: Photocatalytic CO_2 reduction under (a)



prolonged 400 nm LED illumination (ca. 5

$\text{mW}\cdot\text{cm}^{-2}$). (b) AQY for CO production measured at wavelengths shown (red) and overlaid UV/Vis spectrum of the reaction suspension. All experiments are using g- C_3N_4 (urea, 2.5 mg) and CoCl_2 ($50 \mu\text{mol dm}^{-3}$), bpy (5 mmol dm^{-3}) in 5 ml $\text{CH}_3\text{CN}:\text{H}_2\text{O}:\text{TEOA}$, 3:1:1 purged with CO_2 .

Previous hydrogen evolution studies have found that the photocatalytic activity of a platinumized urea derived g- C_3N_4 is significantly greater than other precursor materials.¹⁶ Similarly the highest efficiency material for CO_2 reduction using $[\text{Co}(\text{bpy})_n]^{2+}$ as co-catalyst is g- C_3N_4 (urea), with relative catalytic efficiencies following the trend urea > DCDA > thiourea. The CO yield from g- C_3N_4 (urea) was 5x higher than that from DCDA-derived g- C_3N_4 , and 23x higher than that from thiourea-derived g- C_3N_4 , Table 1. The CO/H_2 selectivity was also 3.3x or 13.3x higher, respectively. Interestingly the relative enhancements in activity for CO_2 reduction reported here are similar to those reported for H_2 production using g- $\text{C}_3\text{N}_4/\text{Pt}$, where g- C_3N_4 (urea) produces H_2 at a rate of 8x relative to g- C_3N_4 (DCDA) and 13.5x relative to g- C_3N_4 (thiourea).¹⁶ In order to benchmark the activity of the urea derived system for CO_2 reduction we have recorded the AQY, also known as the photonic efficiency,²⁶ at a range of wavelengths (Fig. 1 (b)). The AQY response of g- C_3N_4 (urea) and $[\text{Co}(\text{bpy})_n]^{2+}$ matches well to the recorded UV/Vis spectrum of g- C_3N_4 . Direct comparison of efficiencies between this study and others by AQY is complicated as the AQY does not take into account the number of photons absorbed, only those incident on the sample (see ESI for the calculations). However it is apparent that the activity of the urea g- C_3N_4 is at the same level of greater than current state-of-the-art g- C_3N_4 (melamine)/ $\text{CoO}_x/[\text{Co}(\text{bpy})_n]^{2+}$ systems for CO_2 reduction which utilised a ten-fold more concentrated solution of g- C_3N_4 to achieve a maximum AQY of 0.25 % at 420 nm and noted only a small increase in activity at 400 nm.¹⁸ In contrast here we reach a maximum AQY of

1.6 % at 400 nm and at 420 nm, a wavelength where incomplete light harvesting occurs in our reactor (Fig. 1 (b)), an AQY 0.25 % is also achieved. The maximum AQY of 1.6 % is indeed comparable to other state of the art CO₂ reduction photocatalysts.^{20, 27, 28}

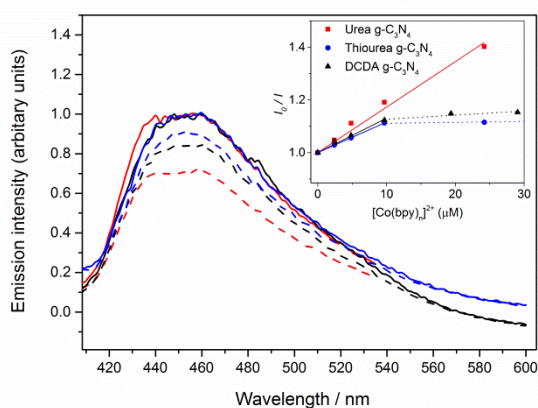
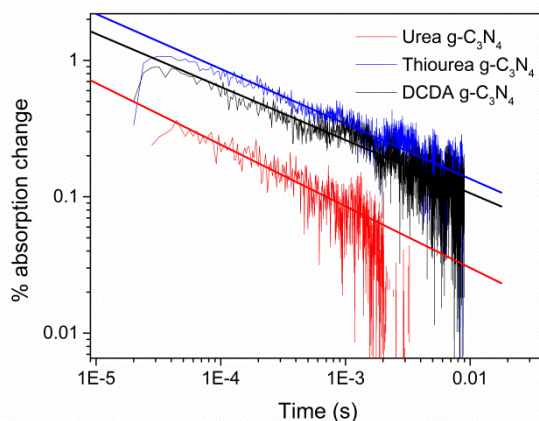


Fig. 2: Normalised emission of urea (red), DCDA (black) and thiourea (blue) derived g-C₃N₄ (0.1 mg ml⁻¹ in 1:1 CH₃CN/H₂O) in the absence of a quencher (solid lines) and relative quenching in the presence of [Co(bpy)₃]²⁺ (dashed lines). Inset shows the Stern-Volmer plots for g-C₃N₄ in CH₃CN/H₂O with a [Co(bpy)₃]²⁺ quencher.

It is striking that the relative trends for the activity of urea, DCDA and thiourea derived g-C₃N₄ are the same for both CO₂ reduction and H₂ evolution.¹⁶ This change in activity cannot be attributed to improved light harvesting of the urea derived material as it displays a wider band gap than both the DCDA and thiourea samples (Table 1, Fig. S4). The photocatalytic CO₂ activity also does not scale linearly with the relative BET surface areas of the materials, Table 1. It has been previously noted that the activity for the different materials for hydrogen evolution correlates with the degree of material hydrogenation (i.e.: the ratio of surface sp² nitrogen sites (C-N-C) to sp³ sites (H-N-[C]₃ and C-NH_x)).¹⁶ DFT calculations indicated that two possible enhancement routes were occurring in materials with high sp²:sp³ ratios. Firstly the observed **wider** band gap of urea derived g-C₃N₄ leads to a raising of the conduction band edge (Fig. S4), which will increase the driving force for electron transfer to any co-catalyst. Secondly a greater level of exciton delocalization was proposed to occur in g-C₃N₄ (urea), minimizing fast exciton recombination and increasing the yield of separated charges which are required for photocatalysis to occur.¹⁶ Here we have explored the potential role of both effects in the photocatalytic CO₂ reduction system. Photoluminescence (PL) occurs in g-C₃N₄ after bandgap excitation due to electron-hole recombination, displaying maxima ranging from 440 – 460 nm. In the presence of an electron acceptor it is known that this emission can be quenched by electron transfer to [Co(bpy)₃]²⁺.¹⁸ Quenching studies in the absence and presence of [Co(bpy)₃]²⁺ were performed (Fig. 2). A Stern-Volmer (SV) plot shows a good linear response for concentrations of co-catalyst up to 10 μmol dm⁻³. Notably the slopes of the SV plots yielded *K_{SV}* constants (see Table S2) with values following the sequence urea > DCDA > thiourea, which mirrors the sequence of photocatalytic activity (transient emission studies indicate a similar lifetime for the emissive states in all three materials, Fig. S5), **and the driving force for electron transfer calculated by DFT and TD-DFT previously.**¹⁶ We also note that for thiourea and DCDA derived g-C₃N₄ no additional quenching occurs at [Co(bpy)₃]²⁺ concentrations above 10 μmol dm⁻³. The lack of linearity at higher quenching concentrations may indicate a population of inaccessible emissive states.²⁹ In DCDA and thiourea derived

materials it is proposed that a significant population of photogenerated charges are trapped at sites inaccessible to the solution, hence making them photochemically less active. In contrast the urea derived $g\text{-C}_3\text{N}_4$ displays reasonable linearity at quencher concentrations up to $24 \mu\text{mol dm}^{-3}$, it is apparent therefore that both the increased driving force for electron transfer from the conduction band of urea derived $g\text{-C}_3\text{N}_4$ to the $[\text{Co}(\text{bpy})_n]^{2+}$ catalyst and the greater accessibility to the $g\text{-C}_3\text{N}_4$ surface are important factors behind the enhanced photocatalytic



activity of this material.

Fig. 3: DR-TA kinetic traces recorded at 850 nm for the $g\text{-C}_3\text{N}_4$ sample indicated under an Argon atmosphere, following UV (355 nm, $91 \mu\text{J}\cdot\text{cm}^{-2}$) excitation.

Transient absorption (TA) spectroscopy is a powerful tool to probe the change in concentration of charge carriers (photogenerated electrons and holes) with time³⁰ and here we also examine the diffuse reflectance TA kinetics of the $g\text{-C}_3\text{N}_4$ samples. Recently it has been highlighted that long-lived photogenerated charges can persist in $g\text{-C}_3\text{N}_4$ into the milliseconds timescales and it has been proposed that these are important in controlling photocatalytic efficiency.^{22, 31} Following UV (355 nm, 6 ns pulse, $91 \mu\text{J}\cdot\text{cm}^{-2}$) excitation we observe a broad long-lived feature in the visible/NIR region that persists for significantly longer timescales (signals remain at > 10 ms after excitation at 850 nm) than the strong emission that is observed between 400 – 600 nm (lifetime ca. 8 ns, Fig. S5). Again a clear trend between the different $g\text{-C}_3\text{N}_4$ samples is noted with the urea derived sample having a far lower yield of long-lived TA features when compared to the DCDA and thiourea samples. DR-TA data spanning the visible-NIR region are also presented in Fig. S6, which show peaks centred around 500 and 850 nm. In recent studies similar $g\text{-C}_3\text{N}_4$ TA features in the visible region have been assigned to trapped electrons or potentially electron-hole pairs and the same assignment is proposed here.^{22, 32, 33} The decay kinetics of the TA features at 850 nm are found to be well fitted by a power law model ($\% \text{abs} \propto t^{-\beta}$, $\beta = 0.42 \pm 0.05$) for all three $g\text{-C}_3\text{N}_4$ samples studied which is likely to indicate that charge recombination is occurring via a trap-detrap mechanism, Fig. 3.³⁴ The weaker long-lived TA signals in our most active photocatalyst is perhaps surprising as it is often suggested that the ability to generate higher yields of long-lived charges is a characteristic of the most active semiconductor photocatalysts.³⁵ Indeed in a recent study on photoelectrochemical water splitting using a protonated $g\text{-C}_3\text{N}_4$ embedded in Nafion such a trend was noted; however it is important to highlight in this case water oxidation was studied and the protonated sample actually had a lower $\text{sp}^2 \text{N}/\text{sp}^3$ ratio than the untreated $g\text{-C}_3\text{N}_4$.³¹ In contrast a recent TA study of $g\text{-C}_3\text{N}_4$ by Kuriki *et al.*²² reported the presence of deeply trapped inactive charges in the visible region. Therefore, in light of the (i) observed trap-mediated recombination kinetics (ii) the inverse

correlation between photocatalytic activity and long-lived charge TA signal and (iii) the previous observation in the emission quenching study of inaccessible sites on DCDA/thiourea g-C₃N₄ we propose that the transient absorption observed here at 850 nm also correlates to deep lying, kinetically less reactive, photogenerated charges. The DCDA and thiourea samples appear to have a higher density of deep lying less photochemically active trap states than the urea derived material which is leading to decreased photocatalytic activity for both CO₂ reduction and hydrogen evolution

Conclusions

We have tested a family of g-C₃N₄ polymers, previously shown to be excellent photocatalysts for H₂ production¹⁶ for CO₂ reduction using [Co(bpy)_n]²⁺ as co-catalyst. This has led to us achieving a five-fold increase in the CO evolution rate. Given that urea derived g-C₃N₄ with a high sp² N: sp³ ratio appears to be generally extremely active for photochemical reductions it is important that the factors controlling activity are resolved. Our TA and emission studies show that an increased driving force for charge transfer to a co-catalyst (in this case [Co(bpy)_n]²⁺) or to a sacrificial electron donor is a significant factor. Perhaps surprisingly we also find that the high activity of the urea derived materials correlates with a lower yield of long-lived deeply trapped photogenerated charges, highlighting the importance of defect and other potential charge trap sites in controlling the photochemistry of g-C₃N₄.

Notes and references

JJW and AJC acknowledge the EPSRC (EP/K006851/1) for a funding and a fellowship respectively and for equipment funding (EP/K031511/1). Thanks to Prof. Dave J. Adams and Prof. Dmitry Shchukin (UoL) for providing access to the fluorimeter and FTIR spectrometer, respectively. Thanks to Mr. Mark Forster (UoL) for his help with DR-TA experiments

Reference

1. S. J. a. Moniz, S. a. Shevlin, D. J. Martin, Z.-X. Guo and J. Tang, *Energy Environ. Sci.*, 2015, **00**, 1–29.
2. X. Wang, K. Maeda, A. Thomas, K. Takanabe, G. Xin, J. M. Carlsson, K. Domen and M. Antonietti, *Nat. Mater.*, 2009, **8**, 76–80.
3. J. Liu, Y. Liu, N. Liu, Y. Han, X. Zhang, H. Huang, Y. Lifshitz, S. Lee, J. Zhong and Z. Kang, 2015, **0006709**, 1–6.
4. J. Hong, S. Yin, Y. Pan, J. Han, T. Zhou and R. Xu, *Nanoscale*, 2014, **6**, 14984–90.
5. L. Shi, L. Liang, F. Wang, M. Liu, K. Chen, K. Sun, N. Zhang and J. Sun, *ACS Sustain. Chem. Eng.*, 2015, **3**, 3412–3419.
6. S. Min and G. Lu, *J. Phys. Chem. C*, 2012, **116**, 19644–19652.
7. X. Zhang, L. Yu, C. Zhuang, T. Peng, R. Li and X. Li, *ACS Catal.*, 2014, **4**, 162–170.
8. Y. Shiraishi, Y. Kofuji, S. Kanazawa, H. Sakamoto, S. Ichikawa, S. Tanaka and T. Hirai, *Chem. Commun.*, 2014, **50**, 15255–15258.
9. C. A. Caputo, M. A. Gross, V. W. Lau, C. Cavazza, B. V. Lotsch and E. Reisner, 2014.
10. X. Wang, G. Zhang, S. Zang, Z. Lan, C. Huang and G. Li, *J. Mater. Chem. A*, 2015, **3**, 17946–17950.
11. G. Dong, Y. Zhang, Q. Pan and J. Qiu, *J. Photochem. Photobiol. C Photochem. Rev.*, 2014, **20**, 33–50.
12. A. Thomas, A. Fischer, F. Goettmann, M. Antonietti, J.-O. Müller, R. Schlögl and J. M. Carlsson, *J. Mater. Chem.*, 2008, **18**, 4893.
13. S. W. Hu, L. W. Yang, Y. Tian, X. L. Wei, J. W. Ding, J. X. Zhong and P. K. Chu, *Appl. Catal. B Environ.*, 2015, **163**, 611–622.
14. K. Takanabe, K. Kamata, X. Wang, M. Antonietti, J. Kubota and K. Domen, *Phys. Chem. Chem. Phys.*, 2010, **12**, 13020–13025.
15. D. J. Martin, P. J. T. Reardon, S. J. a Moniz and J. Tang, *J. Am. Chem. Soc.*, 2014, 2–5.

- 16 D. J. Martin, K. Qiu, S. A. Shevlin, A. D. Handoko, X. Chen, Z. Guo and J. Tang, *Angew. Chemie - Int. Ed.*, 2014, **53**, 9240–9245.
- 17 Y. Zheng, L. Lin, X. Ye, F. Guo and X. Wang, *Angew. Chemie - Int. Ed.*, 2014, **53**, 11926–11930.
- 18 J. Lin, Z. Pan and X. Wang, *ACS Sustain. Chem. Eng.*, 2014, **2**, 353–358.
- 19 J. Lin, Y. Hou, Y. Zheng and X. Wang, *Chem. - An Asian J.*, 2014, **9**, 2468–2474.
- 20 K. Maeda, K. Sekizawa and O. Ishitani, *Chem. Commun. (Camb.)*, 2013, **49**, 10127–9.
- 21 R. Kuriki, K. Sekizawa, O. Ishitani and K. Maeda, *Angew. Chemie - Int. Ed.*, 2015, **54**, 2406–2409
22. R. Kuriki, H. Matsunaga, T. Nakashima, K. Wada, A. Yamakata, O. Ishitani and K. Maeda, *J. Am. Chem. Soc.*, 2016, jacs.6b01997.
- 23 J. Lehn and R. Ziessel, 1982, **79**, 701–704.
- 24 R. Ziessel, J. Hawecker and J.-M. Lehn, *Helv. Chim. Acta*, 1986, **69**, 1065–1084.
- 25 J. Grodkowski and P. Neta, *J. Phys. Chem.*, 2000, **104**, 1848–1853.
- 26 H. Kisch and D. Bahnemann, *J. Phys. Chem. Lett.*, 2015, **6**, 1907–1910.
- 27 S. Sato, T. Morikawa, S. Saeki, T. Kajino and T. Motohiro, 2010.
- 28 E. Pastor, F. M. Pesci, A. Reynal, A. D. Handoko, M. Guo, X. An, A. J. Cowan, D. R. Klug, J. R. Durrant and J. Tang, *PhysChem. Chem. Phys.*, 2014, **16**, 5922–6.
- 29 J. R. Lakowicz, *Principles of Fluorescence Spectroscopy Principles of Fluorescence Spectroscopy*, 2006.
- 30 A. J. Cowan, W. Leng, P. R. F. Barnes, D. R. Klug and J. R. Durrant, *Phys. Chem. Chem. Phys.*, 2013, **15**, 8772.
- 31 C. Ye, J. X. Li, Z. J. Li, X. B. Li, X. B. Fan, L. P. Zhang, B. Chen, C. H. Tung and L. Z. Wu, *ACS Catal.*, 2015, **5**, 6973–6979.
- 32 H. Zhang, Y. Chen, R. Lu, R. Li and a Yu, *Phys Chem Chem Phys*, 2016, **18**, 14904–14910.
- 33 H. Kasap, C. A. Caputo, B. C. M. Martindale, R. Godin, V. W.-H. Lau, B. V. Lotsch, J. R. Durrant and E. Reisner, *J. Am. Chem. Soc.*, 2016, **138**, 9183-9192.
- 34 a. J. Cowan, J. Tang, W. Leng, J. R. Durrant and D. R. Klug, *J Phys. Chem. C*, 2010, **114**, 4208–4214.
- 35 A. J. Cowan and J. R. Durrant, *Chem. Soc. Rev.*, 2013, **42**, 2281–93.

TOC

